PAPER

Check for updates

Facile and scaleable transformation of Cu nanoparticles into high aspect ratio Cu oxide nanowires in methanol†

Minkyu Kang,‡[a] Minjun Bae, [iD] ‡[a] Sumin Park,[a] Hwichan Hong,[a] Taehyun Yoo,[a] Yonghwan Kim, [iD] [a] Myeongseok Jang, [iD] [a] Young-Seok Kim*[b] and Yuanzhe Piao [iD] *[ac]

In this work, a facile synthetic route for the preparation of high aspect ratio Cu oxide nanowires is reported. The preparation of the Cu oxide nanowires begins with the generation of pure Cu nanoparticles by inert gas condensation (IGC) method, follows by dispersing the obtained nanoparticles in methanol with the aid of ultrasonication. The mixture is stored at different temperature for the transformation from Cu nanoparticle to Cu oxide nanowires. The influences of the kind of solution, the ratio of methanol to Cu nanoparticle, dispersion time and temperature towards the generation of Cu oxide nanowires are studied in detail. Scanning electron microscopy studies indicate that high aspect ratio Cu oxide nanowires with diameter of a few tens of nanometers and length up to several tens of micrometers could be obtained under proper conditions. The mechanism for the transformation of Cu nanoparticles to Cu oxide nanowires is also investigated.

1. Introduction

One dimensional (1-D) nanoscale materials, such as nanotubes, nanorods, nanobelts, and nanowires, have attracted much research interest for their special morphologies, unique electronic states, chemical and physical properties compared to their bulk size materials.[1–6] Thanks to these properties, 1-D nanomaterials are now widely used in many fields, such as sensors,[7] catalysts,[8] optical devices,[9] and transparent conductive films.[10]

Among the various 1-D nanomaterials, Cu oxide nanowires have been recently studied for various applications, such as field emission devices,[11] gas sensors,[12] biosensors,[13] and solar cells[14] due to their unique physical and chemical properties, including a high optical absorption coefficient, a lower band gap energy, low toxicity and inexpensiveness.

Various synthetic routes for Cu oxide nanowires have been reported such as solution-based synthesis,[15] thermal oxidation technique,[16] and the electrochemical deposition approaches.[17]

In addition, there are many studies on approaches to Cu oxide nanowire synthesis for improved morphology and electrical characteristics.[18–25] Among these methods, the solution-based synthesis is typically accomplished by mixing chemicals with an aqueous solution.[19,20] The advantage of the solution base methods compared to other technique is the tunability of the nanowires morphology by simply controlling experimental conditions.[25]

But, the solution-based method is sensitive to synthesis conditions and requires several additives.[15] Therefore, there are previous research results that spontaneously grow into a wire using nanostructures as precursors.[26,27]

Ren *et al.* have demonstrated the transformation of ordered mesoporous Cu/CuO into porous Cu_2O nanowires in ethanol. They reported that Cu in mesostructures was slowly oxidized by ethanol to assemble Cu oxide nanoparticles, and which are self-assembled into the porous nanowires.[26]

Ji *et al.* studied the spontaneous organization of Cu_2O/CuO core/shell nanowires in ethanol by the oxidation of Cu nanoparticles under ambient conditions. They demonstrated that Cu^{2+} is supplied from Cu nanoparticles and combined with OH^- of ethanol to form $Cu(OH)_2$, which loses water and Cu oxide is formed by the loss of O_2.[27]

Herein, we demonstrate a facile synthetic route for the preparation of high aspect ratio Cu oxide nanowires using as-generated Cu nanoparticles. The preparation of the Cu oxide nanowires begins with the generation of pure Cu nanoparticles by inert gas condensation (IGC) method (Fig. 1a),[28] followed by dispersing the obtained nanoparticles in methanol with the aid of

[a]*Department of Applied Bioengineering, Graduate School of Convergence Science and Technology, Seoul National University, 16229 Suwon-si, Gyeonggi-do, Republic of Korea. E-mail: parkat9@snu.ac.kr*

[b]*Korea Electronics Technology Institute (KETI), 13509 Seongnam-si, Gyeonggi-do, Republic of Korea. E-mail: vis4freedom@keti.re.kr*

[c]*Advanced Institutes of Convergence Technology, Seoul National University, 16229 Suwon-si, Gyeonggi-do, Republic of Korea*

† Electronic supplementary information (ESI) available. See https://doi.org/10.1039/d2ra00510g

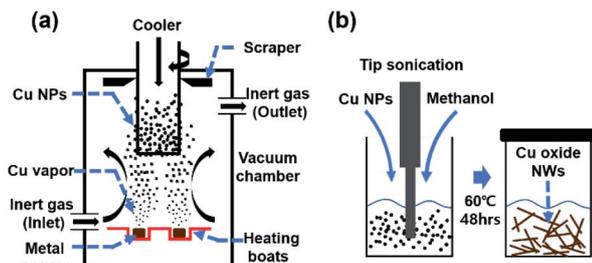‡ These authors contributed equally to this work.

Fig. 1 (a) Schematic diagram of inert gas condensation method for the generation of Cu nanoparticles, (b) transformation from Cu nanoparticles to Cu oxide nanowires.

ultrasonication (Fig. 1b). Previous studies have studied the growth of nanowires with time,[27] but the effect of other factors is required to obtain the morphological uniformity. The optimal conditions to obtain Cu oxide nanowires with uniform morphology were studied by examining the effect of the type of solution, the Cu and solution ratio, time, temperature, the influence of the Cu production method, and the effect of scale-up. Moreover, the potential mechanism for the spontaneous transformation of Cu nanoparticles to Cu oxide nanowires is also proposed.

2. Results and discussion

2.1 Structural characterization of Cu nanoparticles and Cu oxide nanowires

Fig. 2a and b show low and relatively high magnification FE-SEM images of pure Cu nanoparticles generated by the IGC method. The average diameter of prepared Cu nanoparticles is 35 nm with narrow size distribution (Fig. 2c). The diffraction patterns of Cu nanoparticles are shown in Fig. 2d. The XRD pattern of Cu nanoparticles is exactly indexed to crystalline Cu
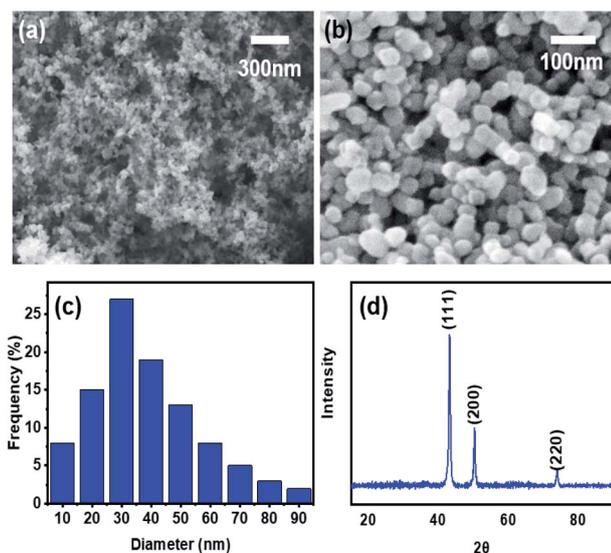

Fig. 2 Low (a) and relatively high (b) magnification FE-SEM images, size distribution (c), and XRD pattern (d) of the generated Cu nanoparticles.

peak (Cubic, Joint Committee on Powder Diffraction Standards (JCPDS) No. 85-1326).

The generated Cu nanoparticles were dispersed in methanol with the aid of ultrasonication without any additives. The ultrasonication of nanoparticles is very effective to decompose large agglomerates containing weakly bound atomic and molecular clusters.[29] The dispersed mixture was observed for change over time (Fig. 3a). Immediately after ultrasonication, the Cu nanoparticles are dispersed in the methanol, and after a few hours, the nanoparticles start to settle down. After 24 hours, the precipitation of dark brown-color particles is observable.

The extended aging time (144 h) results in the continuous growth of nanowires, and the blue particles suspended in the methanol are clearly observable.

We measured the UV-visible absorption of samples at different aging stages according to Fig. 3a. With the increase in the aging time, a new peak at 329 nm appears, which can be attributed to the formation of CuO nanowires (Fig. S1†). In addition, the absorbance spectra between samples at 48 and 144 hours exhibit little difference, which can be attributed to the negligible compositional changes of as-grown CuO nanowires between 48 and 144 hours. In other words, the conversion of Cu nanoparticles to CuO nanowires with high aspect ratio can be complete in 48 hours. The possible mechanism is proposed in the section 2.8.

Further increase in the aging time results in the formation of nanowires with ultrahigh aspect ratios, as confirmed by FE-SEM images (Fig. 3b–f). Cu oxide nanowires with diameter of a few tens of nanometers and length up to several tens of micrometers could be obtained under proper conditions.

As a result of statistical analysis of FE-SEM image, the diameter distribution was confirmed by measuring the diameter for 100 points in the FE-SEM image as shown in Fig. 3e. We performed a statistical analysis of the diameter of CuO nanowires for precise morphological description by using JMP software (Fig. S2†). The average diameter of CuO nanowires is calculated to be 30.2 nm with the standard deviation of 6.18 nm. The minimum and maximum diameters of CuO nanowires are 17.8 and 46.8 nm, respectively. Given the proportions of each group based on the diameter, we can conclude that the morphology of as-prepared CuO nanowires is uniform.

Since no precursor particles were found after 144 h, we assume that all nanoparticles contributed to the transformation into nanowires. It was confirmed that the volume increased as precipitate nanoparticles are transferred into nanowires.

2.2 Influence of utilized solvent on nanoparticle morphology

The as-generated Cu nanoparticles were dispersed in mild solutions for use as metal ink and the changes in morphology during aging time were studied. In previous studies,[26,27] it is possible to confirm the results of spontaneous self-organization of nanowires when dispersed in ethanol. Fig. 4 shows FE-SEM images of the samples obtained from (Fig. 4a and d) methanol (Fig. 4b and e), ethanol, and (Fig. 4c and f) deionized (DI) water. Cu nanoparticles was first dispersed in each liquid with a fixed weight ratio of 1 : 100. After ultrasonication for 5 min,
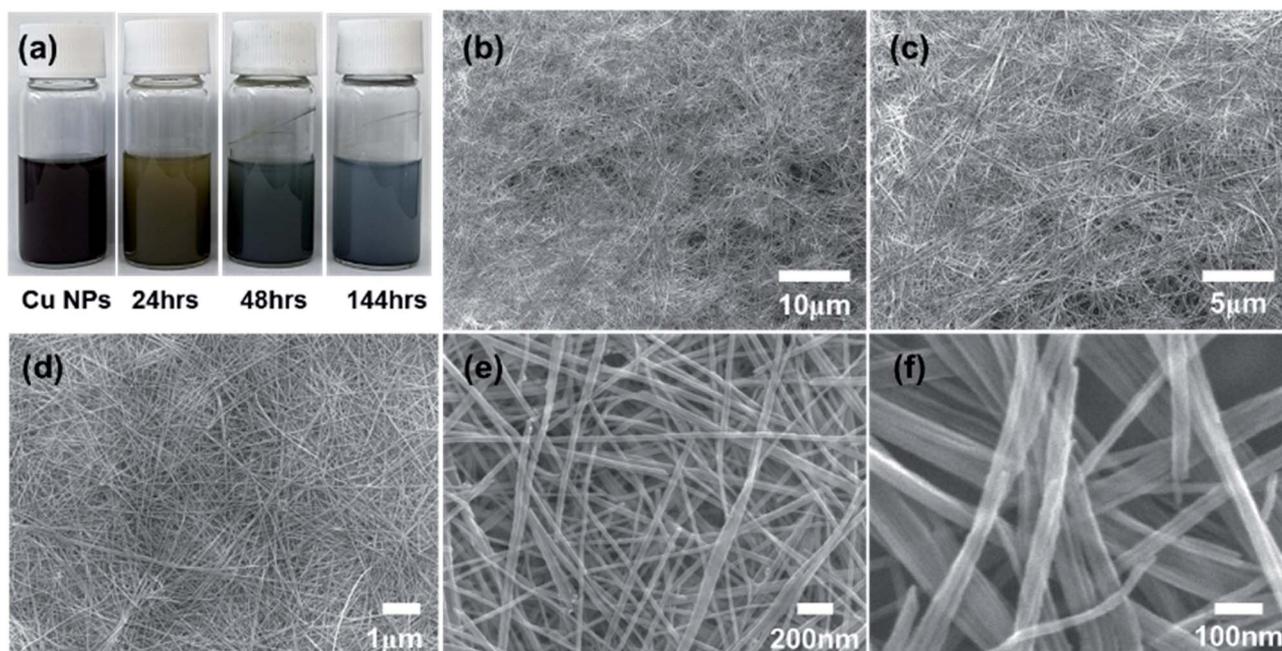
Fig. 3 (a) Photograph of the mixture sample captured at different times (from left to right: immediately after ultrasonication, kept at 60 °C for 24 h, 48 h, and 144 h after ultrasonication). Low (b–d) and relatively high (e and f) magnification FE-SEM images of the CuO nanowires after keeping for 6 days. The weight ratio of Cu nanoparticles to methanol in the mixture is 1 : 2000.
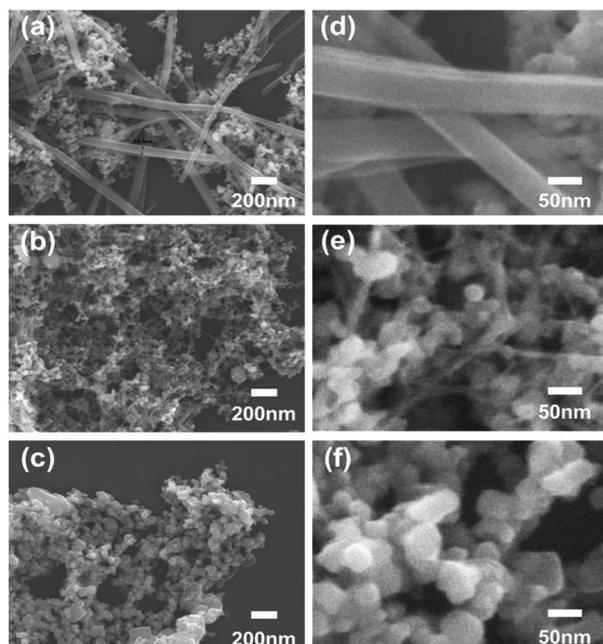

Fig. 4 FE-SEM images of the samples obtained from (a and d) methanol, (b and e) ethanol, and (c and f) DI water. Cu nanoparticles was first dispersed in each liquid with a fixed weight ratio of 1 : 100. After ultrasonication for 5 min, these samples were kept stable at room temperature for 24 h.

these samples were kept stable at room temperature for 24 h. FE-SEM measurements confirmed that Cu nanoparticles in methanol and ethanol are changed to nanowires, while the sample in DI water shows no morphology change. Compared

with the sample in ethanol, nanowires generated in methanol show good straightness and high aspect ratio.

2.3 The effect of Cu nanoparticles/methanol weight ratio on the growth of Cu oxide nanowires

Cu nanoparticles was first dispersed in methanol with different weight ratio. After ultrasonication for 5 minutes, these samples were kept stable at room temperature for 24 hours. It is essential to know the optimal weight ratio on the growth of Cu oxide nanowires. Fig. 5 shows typical FE-SEM images of the samples obtained from different Cu nanoparticles to methanol weight ratio of 1 : 20, 1 : 50, 1 : 100, 1 : 500, 1 : 2000, and 1 : 5000 (Fig. 5a–f). The diameter of each sample (Fig. 5b–f) was 90, 74, 60, 38, and 20 nm, respectively. As shown in Fig. 5a and h, with a high weight ratio of 1 : 20, nanoparticles failed to grow into the nanowires. Fig. 5g presents the relationship between the diameter of the generated nanowires and the weight ratio of Cu nanoparticles to methanol. It was confirmed that a low weight ratio of nanoparticle to methanol leads to a smaller diameter with a high aspect ratio.

2.4 The effects of aging time and temperature on the frequency of nanowires

Since the aging time and aging temperature also alter the growth kinetics, we vary these factors to obtain a deeper understanding of the growth mechanism (Fig. 6). No nanowires were observed at low temperature of 4 °C after 2 hours (Fig. 6a) and the contents of nanowires grown from nanoparticles is only 12% even after 48 hours. In contrast, the growth rate is increased at higher temperature. When the growth was made at
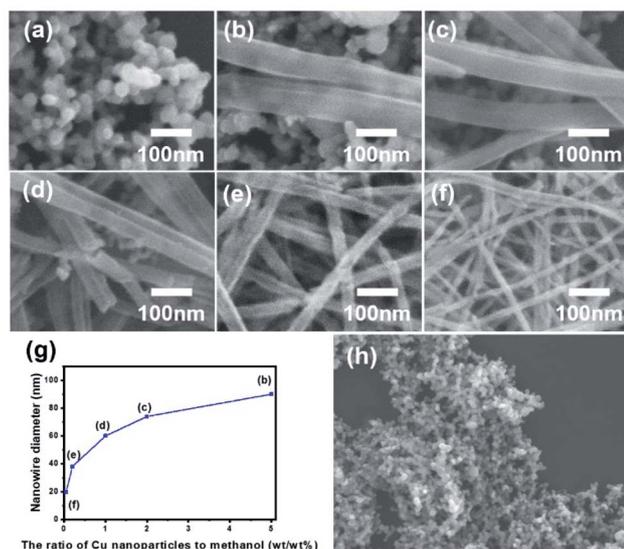
Fig. 5 FE-SEM images of the samples obtained from different Cu nanoparticles to methanol weight ratio of 1 : 20 (a), 1 : 50 (b), 1 : 100 (c), 1 : 500 (d), 1 : 2000 (e), and 1 : 5000 (f). Cu nanoparticles was first dispersed in methanol with different weight ratio. After ultrasonication for 5 min, these samples were kept stable at room temperature for 24 hours. The relationship between the diameter of the generated Cu oxide nanowires and the weight ratio of Cu nanoparticles to methanol (g). Low magnification FE-SEM image of the sample obtained weight ratio of 1 : 20 (h).

60 °C, high-yield nanowires with aspect ratios between 30 and 1000 were obtained. Fig. 6p shows the frequency of nanowires at different temperatures as a function of aging time. The results indicate that the growth rate is strongly influenced by the aging time and temperature, and the transformation of nanoparticles into nanowires at high temperature is accelerated.

2.5   Crystal structure and morphology according to temperature

The structural characteristic and phase purity of the generated Cu oxide nanowires were evaluated by the XRD analysis. Fig. 7

shows the XRD characteristics of the Cu oxide nanowires obtained under aging temperatures of 4 °C, 25 °C and 60 °C. The aging time was fixed for 48 h (corresponding to Fig. 6e, j and o, respectively). Cu (111), (200), and (220) are the only three peaks from pure Cu, which corresponds to Fig. 2d. The result indicates that the particles grown at 4 °C remains the initial crystalline structure. When the aging temperature was raised to 25 °C, Cu_2O peaks (corresponding to 110, 111, 200, 211, 220, and 311) appear, suggesting the successful formation of the Cu_2O nanowires. The CuO phase appears at 60 °C.

Through XRD analysis of the nanowires with different aging temperatures, we can determine that Cu oxide nanowire has a different crystalline structure depending on the aging temperature. As the aging temperature increases, the Cu phase transforms into the Cu_2O phase, and finally into the CuO phase with a preferred orientation of (−111) at 60 °C.[30]

The lattice structure of nanowires was further confirmed by annular bright-field scanning transmission electron microscopy (ABF-STEM) (Fig. 8). The measured nanowires were those grown at 25 °C for 48 hours, which is corresponding to a Fig. 6j sample.
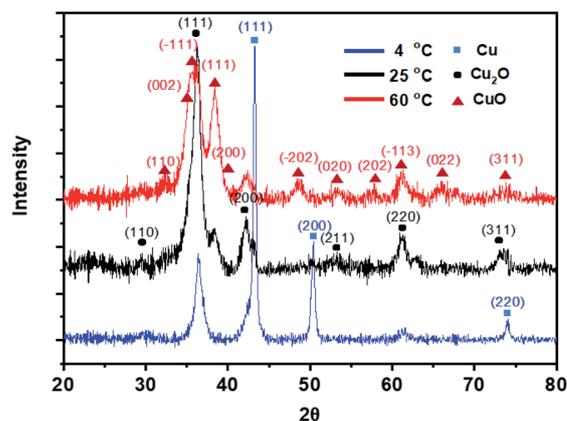

Fig. 7 XRD characteristics of the Cu oxide Nanowires obtained under aging temperatures of 4 °C, 25 °C and 60 °C. The aging time was fixed for 48 h.
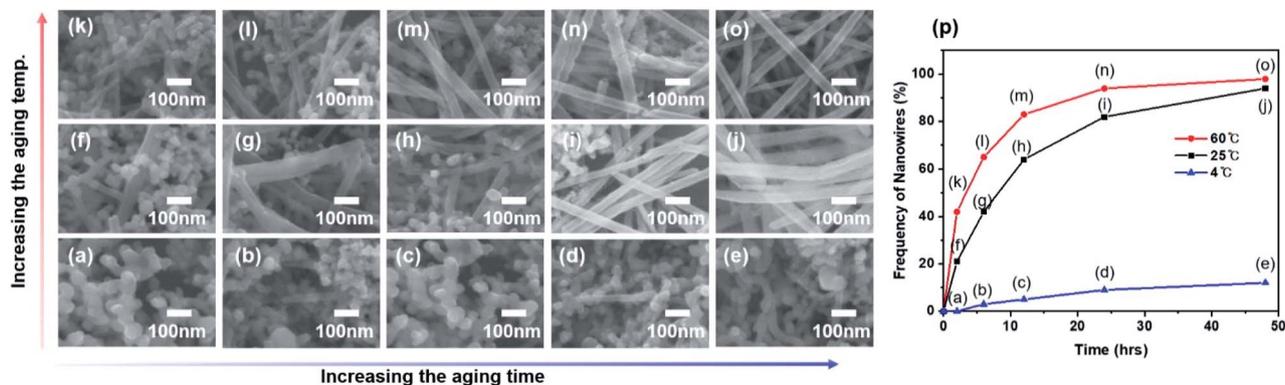

Fig. 6 FE–SEM images of Cu oxide Nanowires obtained with different aging times of 2, 6, 12, 24 and 48 h from left to right. Samples from (a) to (e) were kept as aging temperatures of 4 °C, (f) to (j) at 25 °C, and (k) to (o) at 60 °C. (p) Frequency of nanowires as a function of aging time and temperature. The weight ratio of Cu nanoparticles to methanol in the mixture is 1 : 2000.

RSC Advances

Paper

The investigation of TEM images shows that a single nanowire has a diameter up to 50 nm. The internal structure of nanowires is that crystallites with a size of 5–7 nm are randomly arranged in an amorphous matrix.[20] The crystallites which have a lattice spacing of 0.269 nm and 0.291 nm were randomly oriented in the nanowire. The selected area electron diffraction (SAED) pattern contains multiple sharp diffraction spots and ring patterns as shown in Fig. 8d. These can be matched as (110), (111), (200), (221), (220), and (311) reflections in experimental and simulated SAED pattern compared to polycrystalline Cu_2O.[20]

2.6 The results of scale-up transformation of Cu nanoparticles into nanowires

The preparation of Cu oxide nanowires in large quantities can be useful in various applications, such as secondary batteries,[31] electrocatalysts,[32] thermal transfer medium[33] and so on. Therefore, the potential scalability of Cu nanowires is evaluated by increasing the volume of the synthesis. Fig. 9 shows photographs of the mixture samples for scale-up synthesis captured immediately after ultrasonication (Fig. 9a) and after aging at 60 °C for 48 h (Fig. 9b). FE-SEM image of the sample obtained immediately after ultrasonication is shown as Fig. 9c. Fig. 9d and e show low and relatively high magnification FE-SEM images of the sample obtained after aging at 60 °C for 48 h. The weight ratio of Cu nanoparticles to methanol in these mixtures were all fixed to 1 : 1000. The increased volume of methanol solution and Cu nanoparticles had nearly no effects on morphologies of the generated nanowires, suggesting that the process shown here could be scale-up transformation of Cu nanoparticles into nanowires.
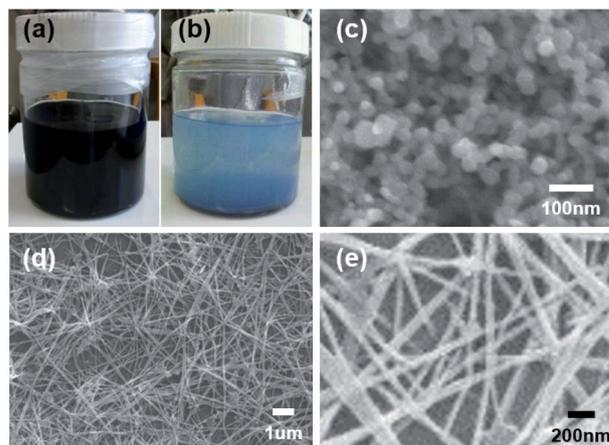

Fig. 9 Photographs of the mixture samples captured immediately after ultrasonication (a), after aging at 60 °C for 48 h (b). FE-SEM images of the samples obtained immediately after ultrasonication (c), low (d) and relatively high (e) images after aging at 60 °C for 48 h. The weight ratio of Cu nanoparticles to methanol in the mixtures were all fixed to 1 : 1000.

2.7 Test of using Cu nanoparticles prepared polyol method for the generation of Cu nanowires

In case of Cu particles generated by the IGC method, it was verified through experiments that Cu nanoparticles were successfully transformed into high aspect ratio Cu oxide nanowires in methanol within a short time. However, the IGC method requires a lot of energy for evaporation and expensive equipment is required to mass-produce nanoparticles.

Since Cu particles could also be made by solution based chemical method, we also prepared Cu nanoparticles by polyol synthetic method and tested the possibility of using these particles as precursor for the synthesis of Cu nanowires.

Fig. 10 summarize the experimental results of using Cu particles made by the polyol method.[34] Fig. 10a shows the FE-SEM image of as-prepared Cu particles with average diameter of 1.5 μm obtained by polyol process. Typical FE-SEM images (Fig. 10b and c) show that even after a long growth period 144 h, only low aspect ratio Cu oxide nanowires are generated. Fig. 10d is a TEM image of the nanowires with a diameter of 50 nm or less. In general, particles made by solution based chemical process is not easy to get pure Cu phase due to easy oxidation of Cu. Additionally, the removal of the surfactant after preparation of nanoparticles by solution based chemical synthesis is time consuming.

The experimental result show that pure Cu nanoparticles with clean surface obtained by IGC method is more suitable for the preparation of high aspect ratio Cu oxide nanowires, and that the morphology varies according to the particle surface condition.

2.8 The growth and transformation mechanism

There are several studies on the growth and transformation mechanism.[26,27] In this work, pure Cu nanoparticles prepared by IGC method were used as precursor material. With IGC method,
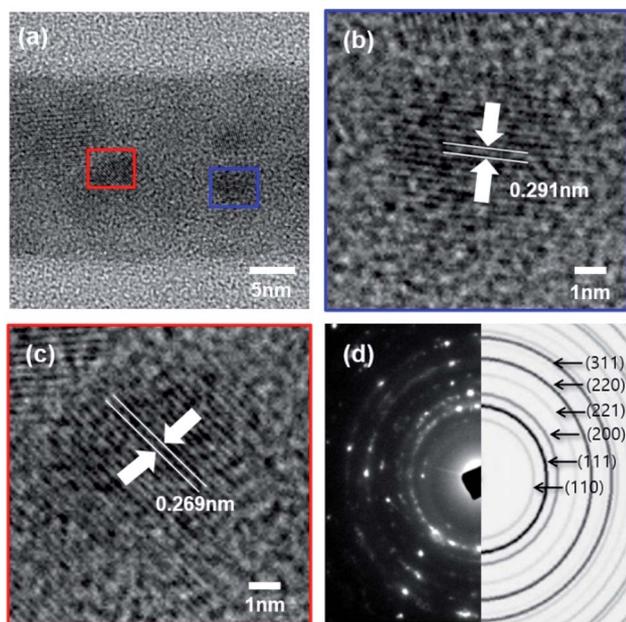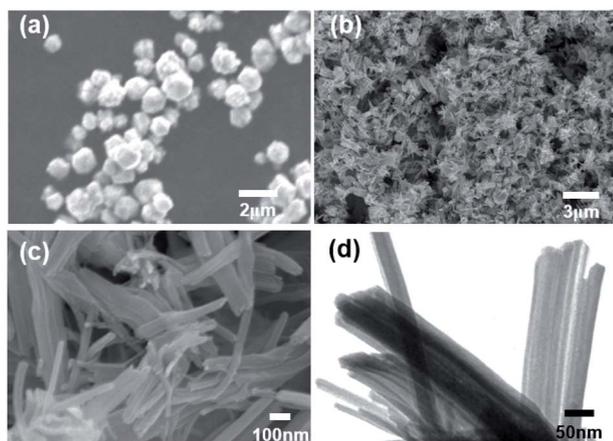

Fig. 8 (a) ABF–TEM image of Fig. 6(j), (b) and (c) crystal lattice spacing, (d) comparison of experimental and simulated SAED patterns of Cu_2O nanowires.
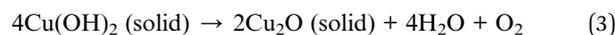
Fig. 10 (a) FE-SEM image of big sized Cu particles obtained by polyol process. Low (b) and relatively high magnification (c) FE-SEM images of Cu oxide nanowires obtained by using the big sized Cu particles. (d) TEM image of the nanowires. The weight ratio of big sized Cu particles to methanol in the mixture was fixed to 1 : 2000. After ultrasonication for 5 min, the sample was kept stable at 60 °C for 144 h.

thermally evaporated Cu rapidly condenses into nanoparticles in which the status is thermodynamically unstable.

These conditions will create many defects on the particle surface and constitute an unstable lattice structure.[35] After dispersing Cu nanoparticles into methanol, the mixture of Cu and methanol was brownish-black in color. And ultrasonication for particle dispersion amplifies the unstable surface state.[36]

Possible transformation mechanism of the Cu to Cu oxide can be described as following.

$$Cu - 2e^- \rightarrow Cu^{2+} \tag{1}$$

$$Cu^{2+} + 2OH^- \rightarrow Cu(OH)_2 \text{ (solid)} \tag{2}$$

$$4Cu(OH)_2 \text{ (solid)} \rightarrow 2Cu_2O \text{ (solid)} + 4H_2O + O_2 \tag{3}$$

$$2Cu_2O \text{ (solid)} + O_2 \rightarrow 4CuO \text{ (solid)} \tag{4}$$

Cu nanoparticles with unstable surface are all ionized into Cu^{2+} and combined with OH^- in methanol to form $Cu(OH)_2$. During the aging process in thermal conditions, $Cu(OH)_2$ loses H_2O molecules and Cu oxide is gradually formed by the release of O_2.[27,37]

Cu nanoparticles gradually dissolved in the methanol solution, and CuO nanowires are simultaneously formed as the reaction progresses (Fig. 11).

The growth mechanism of Cu nanoparticles into CuO nanowires can be explained by surface energies associated with the crystal structure. The XRD pattern of CuO nanowires shown in Fig. 7 exhibits the dominance of (111) and (−111) diffraction peaks of CuO nanowires, indicating the largest exposure of (111) and (−111) crystal facets.[38] According to the previous study, the surface energies of (111) and (−111) crystallographic planes of CuO are the lowest under ambient conditions, which can result in the preferential nucleation on these specific facets.[39] In other words, the growth rate may be accelerated along (111) and (−111)
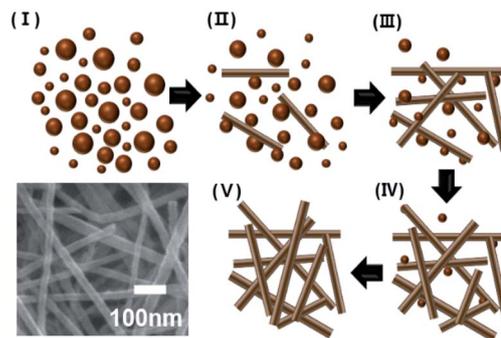
Fig. 11 Schematic diagram for the transformation of Cu nanoparticles into high aspect ratio Cu oxide nanowires (inset is typical SEM image of the generated Cu oxide nanowires).

directions due to lower surface energies, resulting in the anisotropic growth on these facets to form nanowires.[27]

The growth step of Cu oxide nanowires can be explained with metastable phase of $Cu(OH)_2$ used as a precursor. It is considered that methanol and $Cu(OH)_2$ molecules surround the Cu ions and act as a template to grow in the axial direction.[23] In addition, the layered molecular structure of $Cu(OH)_2$ helps the one-dimensional growth.[37] At this point, methanol and $Cu(OH)_2$ can interact with molecular structure through adsorption and desorption to act as a capping agent for the resulting nanowires. It kinetically controls the growth rate in different directions.[40]

Although there is no clear evidence for the capping action of methanol, it is possible that the greater the amount of methanol, the more prominent steric effects and intensive adsorption selectivity.[24]

3. Conclusions

In conclusion, we proposed a facile synthetic route for the preparation of high aspect ratio Cu oxide nanowires. The approach shown in this work is suitable for scale-up synthesis. The as-prepared Cu oxide nanowires show a high aspect ratio and the diameter of the nanowires could be easily controlled by manipulating the aging temperature, aging time and ratio of Cu nanoparticles to methanol. The potential mechanism for the transformation of Cu nanoparticles to Cu oxide nanowires is also proposed. This method is expected to be extended to prepare other nanostructured materials.

4. Experimental

This facile synthetic route can be divided into two major steps: (1) the generation of monodispersed pure Cu nanoparticles by inert gas condensation (IGC) method and (2) follows by dispersing the obtained nanoparticles in methanol with the aid of ultrasonication to convert spherical particles into nanowires.

4.1 Preparation of Cu nanoparticles

Pure Cu nanoparticles were generated by IGC technology (KVT-D665, Korea Vacuum Tech., Ltd) in Fig. 1a shown with

schematic diagram IGC method.[28] Cu (shot, 2–8 mm, 99.9995%, Sigma-Aldrich) and high purity argon gas (99.999%) were used for generation. The process for IGC consists of Cu evaporation inside the chamber that is evacuated to a high vacuum of about 10^{-6} Torr (1 Torr = 133 Pa). Then the chamber was backfilled with argon gas to 0.5 Torr. After evaporation of Cu (evaporation rates: 0.125 g min^{-1}), condensed particles are scraped from the cold finger in an argon gas atmosphere to prevent oxidation.

4.2 Synthesis of Cu oxide nanowires

Cu oxide nanowires were synthesized from the obtained pure Cu nanoparticles and methanol (99.9%, Sigma-Aldrich). The pure Cu nanoparticles are dispersed in methanol with the aid of ultrasonication (VC 750, Sonic & Materials INC.) for 5 minutes. This was done in an argon filled glove box to prevent oxidation of the Cu nanoparticle surface. The mixture is sealed and stored at different aging condition for the transformation from Cu nanoparticle to Cu oxide nanowires.

4.3 Characterization

The nanowire morphologies and structure were characterized by field emission scanning electron microscopy (FE-SEM, JEOL, JSM7000F) and transmission electron microscope (TEM, JEOL, JEM-3010). The crystalline phase of the nanowires was obtained via XRD in 20–80° scans (BRUKER AXS, D8 FOCUS) using Cu K-α radiation (λ = 1.5406 nm). UV spectrum was investigated by PerkinElmer Lambda 35 UV/VIS spectrometer.

Conflicts of interest

There are no conflicts to declare.

Acknowledgements

Notes and references

1 S. Iijima, *Nature*, 1991, **354**, 56–58.
2 J. D. Homes, K. P. Johnston, R. C. Doty and B. A. Korgel, *Science*, 2000, **287**, 1471–1473.
3 Z. W. Pan, Z. R. Dai and Z. L. Wang, *Science*, 2001, **291**, 1947–1949.
4 F. Krumeich, H. J. Muhr, M. Niederberger, F. Bieri, B. Schnyder and R. Nesper, *J. Am. Chem. Soc.*, 1999, **121**, 8324–8331.
5 Y. Xia, P. Yang, Y. Sun, Y. Wu, B. Mayers, B. Gates, Y. Yin, F. Kim and H. Yan, *Adv. Mater.*, 2003, **15**, 353–389.
6 J. Hu, M. Ouyang, P. Yang and C. M. Lieber, *Science*, 1999, **399**, 48–51.
7 Y. Cui, Q. Wei, H. Park and C. M. Lieber, *Science*, 2001, **293**, 1289–1292.
8 X. Xie, Y. Li, Z. Q. Liu, M. Haruta and W. Shen, *Nature*, 2009, **458**, 746–749.
9 X. Duan, Y. Huang, R. Agarwal and C. M. Lieber, *Nature*, 2003, **421**, 241–245.
10 Z. Wu, Z. Chen, X. Du, J. M. Logan, J. Sippel, M. Nikolou, K. Kamaras, J. R. Reynolds, D. B. Tanner, A. F. Hebard and A. G. Rinzler, *Science*, 2004, **305**, 1273–1276.
11 C. T. Hsieh, J. M. Chen, H. H. Lin and H. C. Shin, *Appl. Phys. Lett.*, 2003, **83**, 3383–3385.
12 Y. S. Kim, I. S. Hwang, S. J. Kim, C. Y. Lee and J. H. Lee, *Sens. Actuators, B*, 2008, **135**, 298–303.
13 Z. Zhuang, X. Su, H. Yuan, Q. Sun, D. Xiao and M. M. F. Choi, *Analyst*, 2008, **133**, 126–132.
14 S. Anandan, X. Wen and S. Yang, *Mater. Chem. Phys.*, 2005, **93**, 35–40.
15 W. Wang, G. Wang, X. Wang, Y. Zhan, Y. Liu and C. Zheng, *Adv. Mater.*, 2002, **14**, 67–69.
16 X. Jiang, T. Herricks and Y. Xia, *Nano Lett.*, 2002, **2**, 1333–1338.
17 H. S. Shin, J. Y. Song and J. Yu, *Mater. Lett.*, 2009, **63**, 397–399.
18 L. Yuan, Y. Wang, R. Mema and G. Zhou, *Acta Mater.*, 2011, **59**, 2491–2500.
19 S. Hacialioglu, F. Meng and S. Jin, *Chem. Commun.*, 2012, **48**, 1174–1176.
20 Z. C. Orel, A. Anžlovar, G. Dražić and M. Žigon, *Cryst. Growth Des.*, 2007, **7**, 453–458.
21 W. Wang, L. Wang, H. Shi and Y. Liang, *CrystEngComm*, 2012, **14**, 5914–5922.
22 C. Lu, L. Qi, J. Yang, D. Zhang, N. Wu and J. Ma, *J. Phys. Chem. B*, 2004, **108**, 17825–17831.
23 G. H. Du and G. V. Tendeloo, *Chem. Phys. Lett.*, 2004, **393**, 64–69.
24 Y. Tan, X. Xue, Q. Peng, H. Zhao, T. Wang and Y. Li, *Nano Lett.*, 2007, **7**, 3723–3728.
25 X. Zhang, G. Wang, X. Liu, J. Wu, M. Li, J. Gu, H. Liu and B. Fang, *J. Phys. Chem. C*, 2008, **112**, 16845–16849.
26 Y. Ren, Z. Ma and P. G. Bruce, *CrystEngComm*, 2012, **14**, 2617.
27 J. Y. Ji, P. H. Shih, C. C. Yang, T. S. Chan, Y. R. Ma and S. Y. Wu, *Nanotechnology*, 2010, **21**, 045603.
28 M. K. Kang, J. W. Kim, M. G. Kwak, H. G. Yoon and Y. S. Kim, *J. Nanosci. Nanotechnol.*, 2011, **11**, 6020–6024.
29 J. E. Graves, M. Sugden, R. E. Litchfield, D. A. Hutt, T. J. Mason and A. J. Cobley, *Ultrason. Sonochem.*, 2016, **29**, 428–438.
30 S. Han, H. Y. Chen, Y. B. Chu and H. C. Shih, *J. Vac. Sci. Technol., B: Microelectron. Nanometer Struct.–Process., Meas., Phenom.*, 2005, **23**, 2557.
31 L. Wang, K. Zhang, Z. Hu, W. Duan, F. Cheng and J. Chen, *Nano Res.*, 2014, **7**, 199–208.
32 S. M. Pawar, B. S. Pawar, A. I. Inamdar, J. Kim, Y. Jo, S. Cho, S. S. Mali, C. K. Hong, J. Kwak, H. Kim and H. Im, *Mater. Lett.*, 2017, **187**, 60–63.

33 N. Kana, K. Kaviyarasu, T. Khamliche, C. M. Magdalane and M. Maaza, *J. Environ. Eng.*, 2019, **7**, 103255.

34 Y. Zhang, P. Zhu, G. Li, T. Zhao, X. Fu, R. Sun, F. Zhou and C. Wong, *ACS Appl. Mater. Interfaces*, 2014, **6**, 560–567.

35 M. T. Swihart, *Curr. Opin. Colloid Interface Sci.*, 2003, **8**, 127–133.

36 M. Kamalgharibi, F. Hormozi, S. A. H. Zamzamian and M. Sarafraz, *Heat Mass Transfer*, 2016, **52**, 55–62.

37 Y. Cudennec and A. Lecerf, *Solid State Sci.*, 2003, **5**, 1471–1474.

38 H. Hu, H. Yu, K. Ding, Z. Jiang, Y. Liao, X. Ge, M. Sun and C. Deng, *J. Mater. Sci.: Mater. Electron.*, 2021, **32**, 11989–12000.

39 J. Hu, D. Li, J. G. Lu and R. Wu, *J. Phys. Chem. C*, 2010, **114**, 17120–17126.

40 T. Y. Kim, W. J. Kim, S. H. Hong, J. E. Kim and K. S. Suh, *Angew. Chem., Int. Ed.*, 2009, **48**, 3806–3809.